S_8 increases with effective redshift in ΛCDM cosmology

S. A. Adil,[1] Ö. Akarsu,[2] M. Malekjani,[3] E. Ó Colgáin *,[4] S. Pourojaghi,[5] A. A. Sen [6]
and M. M. Sheikh-Jabbari [5]

[1]*Department of Physics, Jamia Millia Islamia, New Delhi - 110025, India*
[2]*Department of Physics, Istanbul Technical University, Maslak 34469 Istanbul, Turkey*
[3]*Department of Physics, Bu-Ali Sina University, Hamedan 65178, Iran*
[4]*Atlantic Technological University, Ash Lane, Sligo, Ireland*
[5]*School of Physics, Institute for Research in Fundamental Sciences (IPM), P.O.Box 19395-5531, Tehran, Iran*
[6]*Centre for Theoretical Physics, Jamia Millia Islamia, New Delhi - 110025, India*

ABSTRACT

Hubble constant H_0 and weighted amplitude of matter fluctuations S_8 determinations are biased to higher and lower values, respectively, in the late Universe with respect to early Universe values inferred by the Planck collaboration within flat ΛCDM cosmology. If these anomalies are physical, i.e. not due to systematics, they naively suggest that H_0 decreases and S_8 increases with effective redshift. Here, subjecting matter density today Ω_m to a prior, corresponding to a combination of Planck CMB and BAO data, we perform a consistency test of the Planck-ΛCDM cosmology and show that S_8 determinations from $f\sigma_8(z)$ constraints increase with effective redshift. Due to the redshift evolution, a $\sim 3\sigma$ tension in the S_8 parameter with Planck at lower redshifts remarkably becomes consistent with Planck within 1σ at high redshifts. This provides corroborating support for an S_8 discrepancy that is physical in origin. We further confirm that the flat ΛCDM model is preferred over a theoretically ad hoc model with a jump in S_8 at a given redshift. In the absence of the CMB+BAO Ω_m prior, we find that $> 3\sigma$ tensions with Planck in low redshift data are ameliorated by shifts in the parameters in high redshift data. Results here and elsewhere suggest that the ΛCDM cosmological parameters are redshift dependent. Fitting parameters that evolve with redshift is a recognisable hallmark of model breakdown.

Key words: cosmological parameters, large-scale structure of Universe

1 INTRODUCTION

Modern cosmology is a pursuit where one theoretically guesses a function (or model) and compares it to another *a priori* unknown function, the Hubble parameter $H(z)$, extracted observationally from Nature. Given the possibilities, the guess is invariably wrong, but existing cosmological data can mask disagreement until precision improves. Viewed historically, concordance Lambda cold dark matter (ΛCDM) cosmology emerged when a spatially flat, homogeneous & isotropic Universe, filled exclusively with radiation and (pressure-less) matter, required a dark energy sector to explain observations Riess et al. (1998); Perlmutter et al. (1999). Further improvements in data in recent years have unveiled anomalies in the Hubble constant $H_0 := H(z = 0)$ Aghanim et al. (2020); Riess et al. (2022); Freedman (2021); Pesce et al. (2020); Blakeslee et al. (2021); Kourkchi et al. (2020), the weighted amplitude of matter fluctuations $S_8 := \sigma_8 \sqrt{\Omega_m/0.3}$ Aghanim et al. (2020); Heymans et al. (2013); Joudaki et al. (2017); Troxel et al. (2018); Hikage et al. (2019); Asgari et al. (2021); Abbott et al. (2022), the lensing parameter A_{lens} and/or curvature Ω_k Aghanim et al. (2020); Addison et al. (2016); Handley (2021); Di Valentino et al. (2019), the late-time integrated Sachs-Wolfe (ISW) effect Granett et al. (2008); Kovács et al. (2017,

2019, 2022), and high redshift galaxies that seemingly defy ΛCDM expectations Adams et al. (2022); Labbé et al. (2023); Castellano et al. (2022); Naidu et al. (2022). See Di Valentino et al. (2021); Perivolaropoulos & Skara (2022); Abdalla et al. (2022) for reviews of ΛCDM anomalies. It is plausible that the (flat) ΛCDM cosmological model is breaking down. What remains is to confirm this diagnosis.

To that end, a simple insight comes directly to us from the Friedmann equations; H_0 is by construction an integration constant. In other words, it is *theoretically* a constant within the Friedmann-Lemaître-Robertson-Walker (FLRW) framework on which ΛCDM is established by assuming spatial flatness. Nevertheless, it is *observationally* a constant only when one has the correct cosmological model Krishnan et al. (2021); Krishnan & Mondol (2022). This statement is true not only for H_0, but also for other model parameters that are integration constants, such as matter density parameter (today) $\Omega_m := \rho_{m0}/3H_0^2$ (ρ_{m0} being the matter energy density today) in the ΛCDM model. Thus, if the ΛCDM model is breaking down, as all cosmological models must at some precision for the reason outlined above, one expects H_0, Ω_m, etc, to evolve with effective redshift. There are now numerous observations suggesting that H_0 evolves, more accurately decreases with effective redshift Wong et al. (2020); Millon et al. (2020); Krishnan et al. (2020); Dainotti et al. (2021, 2022); Ó Colgáin et al. (2022); Ó Colgáin et al. (2022); Malekjani

* E-mail: eoin.ocolgain@atu.ie

et al. (2023) (see also Hu & Wang (2022); Jia et al. (2023)). Likewise there are claims of Ω_m increasing with effective redshift Ó Colgáin et al. (2022); Ó Colgáin et al. (2022); Malekjani et al. (2023) (see also Risaliti & Lusso (2019); Lusso et al. (2020); Yang et al. (2020); Khadka & Ratra (2020, 2021, 2022); Pourojaghi et al. (2022); Pastén & Cárdenas (2023)). Furthermore, it has been noted in Ó Colgáin et al. (2022); Ó Colgáin et al. (2022); Malekjani et al. (2023) that evolution of H_0 and Ω_m within ΛCDM are anti-correlated with each other. Note that if Ω_m evolves with effective redshift, it is unlikely that S_8 is a constant, because σ_8 conspiring to balance evolution in Ω_m represents a contrived or unnatural scenario.

Here we focus on the S_8 discrepancy Aghanim et al. (2020); Heymans et al. (2013); Joudaki et al. (2017); Troxel et al. (2018); Hikage et al. (2019); Asgari et al. (2021); Abbott et al. (2022). Taken at face value, this anomaly says that S_8 as inferred by the Planck collaboration (high redshift inference) has a larger value than galaxy surveys (low redshift measurement). This can be independently verified with growth rate data, in particular measurements of $f\sigma_8(z)$, which are independent of galaxy bias. Concretely, we will assume expressions that are valid for ΛCDM cosmology and fit $f\sigma_8(z)$ constraints in a single bin of increasing effective redshift. However, since growth rate data suffers from large fractional errors, we will leverage a working assumption in modern cosmology that Ω_m is tightly constrained to elucidate the trend. This means that the increases observed in S_8 are driven by increases in σ_8. Interestingly, this effect is also evident when one compares σ_8 constraints from number counts of galaxy clusters identified through the Sunyaev-Zeldovich effect at low redshifts with σ_8 constraints from Lyman-α spectra at high redshifts Esposito et al. (2022). Moreover, CMB lensing, an observable most sensitive to redshift ranges $z \in [0.5, 5]$ and peaking in sensitivity at $z \sim 2$, recovers the Planck result Qu et al. (2023); Madhavacheril et al. (2023). This seemingly constrains any "S_8 tension" to the late Universe Marques et al. (2023) [1]. Admittedly, Ω_m may not be a constant Ó Colgáin et al. (2022); Ó Colgáin et al. (2022), but this is currently a fringe viewpoint. While S_8 or σ_8 tension in growth rate data is well studied in the literature Macaulay et al. (2013); Battye et al. (2015); Nesseris et al. (2017); Kazantzidis & Perivolaropoulos (2018); Skara & Perivolaropoulos (2020); Quelle & Maroto (2020); Li et al. (2021); Benisty (2021); Nunes & Vagnozzi (2021), our goal in this letter is to explore redshift evolution of S_8 within ΛCDM in the late Universe under standard assumptions.

2 WARM UP

To get oriented, we impose a Gaussian prior, $\Omega_m = 0.3111 \pm 0.0056$, which arises from combining Cosmic Microwave Background (CMB), galaxy, quasar and Lyman-α baryon acoustic oscillation (BAO) constraints Aghanim et al. (2020); Alam et al. (2017); Hou et al. (2020); Neveux et al. (2020). In line with standard practice, we assume there is no discrepancy between CMB and BAO on Ω_m inferences, i. e. that the key success of the ΛCDM model is not undermined. The CMB+BAO prior is needed to compensate for the relatively low quality of the growth rate data, which will be further reduced by the removal of low redshift data. Compared to Planck Aghanim et al. (2020), our constraint is marginally more constraining, but remains representative of a Planck prior. In the absence of Gaussian priors, we employ uninformative uniform priors

$\Omega_m \sim \mathcal{U}(0, 1)$ and $\sigma_8 \sim \mathcal{U}(0, 1.5)$ throughout. We combine this prior with 20 measurements of $f\sigma_8(z)$ from peculiar velocity and redshift-space distortion (RSD) data Said et al. (2020); Beutler et al. (2012); Huterer et al. (2017); Boruah et al. (2020); Turner et al. (2022); Blake et al. (2011, 2013); Howlett et al. (2015); Okumura et al. (2016); Pezzotta et al. (2017); Alam et al. (2021), as compiled recently in Nguyen et al. (2023). Modulo the removal of low redshift data, we follow the methodology of Nguyen et al. (2023). We illustrate the constraints in Fig. 1 in red. We will be interested in the combination

$$S_8 := \sigma_8 \sqrt{\Omega_m/0.3}, \tag{1}$$

where the constant σ_8 is the amplitude of matter fluctuations in spheres of $8h^{-1}$ Mpc with $h := H_0/100\,\text{km s}^{-1}\text{Mpc}^{-1}$. Following Wang & Steinhardt (1998), we introduce the matter density parameter,

$$\Omega(z) := \frac{\Omega_m(z)}{H(z)^2/H_0^2} = \frac{\Omega_m(1+z)^3}{1 - \Omega_m + \Omega_m(1+z)^3}, \tag{2}$$

thereby allowing us to obtain

$$f\sigma_8(z) = \sigma_8\, \Omega^{\frac{6}{11}}(z) \exp\left(-\int_0^z \frac{\Omega^{\frac{6}{11}}(z')}{1+z'}\mathrm{d}z'\right). \tag{3}$$

As explained in Wang & Steinhardt (1998), these expressions are a valid approximation for ΛCDM. Concretely, we checked that the fractional error between the approximation and the exact expression for $f\sigma_8(z)$ based on the hypergeometric function ${}_2F_1$ (see Nesseris et al. (2017)) is greatest at 1% at $z = 0$. In the range $0.35 \lesssim z \lesssim 2$, the fractional error is less than 0.2%. This uncertainty is negligible compared to the observational uncertainties in Fig. 1. Working with an approximation may seem obsolete, but it allows us to shed light on evolution that is hidden in the analysis of Nguyen et al. (2023) [2], where the same approximation and data are employed. For all redshifts z, the function $\Omega(z)$ is bounded $\Omega_m \le \Omega(z) < 1$. In particular, $\Omega \to 1$ as $z \to \infty$, so that Ω_m dependence drops out as an overall factor in (3) at high redshifts, but some knowledge of Ω_m is retained through the integral. Thus, one expects Ω_m to be poorly constrained at higher redshifts. As we show in the appendix, one risks encountering a degeneracy between the fitting parameters (Ω_m, σ_8) that is difficult to cleanly break with exclusively high redshift binned data. Mathematically, one is guaranteed to run into a problem constraining Ω_m in high redshift bins, so it is prudent to impose an Ω_m prior. Later we will relax the prior and comment on the changes.

The green curve in Fig. 1 denotes the best fit of the ΛCDM model to the 20 data points, whereas the blue curve documents the effect of introducing the Gaussian prior on Ω_m. It is worth noting that this increases the S_8 inference and visibly worsens the fit to the $f\sigma_8(z)$ constraints at $z \approx 0$ and $z \approx 1.5$, thereby underscoring the tension between the Ω_m prior and the lower value of Ω_m preferred by $f\sigma_8(z)$ data. The blue curve worsens the fit to $f\sigma_8(z)$ data by $\Delta\chi^2 \approx 4.9$. The $f\sigma_8(z)$ constraints are weak while the Gaussian prior is strong. Therefore, the prior effectively fixes Ω_m, so that the only parameter being fitted is σ_8. As is clear from (3), one is simply fitting the scale of the $f\sigma_8(z)$ function, whereas the functional form is fixed. In Fig. 2 we see the effect of removing $f\sigma_8(z)$ constraints below $z = z_{\min}$. We see that with Ω_m constrained through the prior, σ_8 increases leading to larger values of S_8. As S_8 increases, the curves visibly provide a better fit to high redshift $f\sigma_8(z)$ constraints. This increase in S_8 is

---

[1] Intriguingly, higher redshift observables may prefer lower values of σ_8 relative to Planck Miyatake et al. (2022); Alonso et al. (2023). Ω_m is poorly constrained at high redshifts.

[2] In Nguyen et al. (2023) it is assumed that there is no evolution in cosmological parameters across the $f\sigma_8(z)$ constraints.
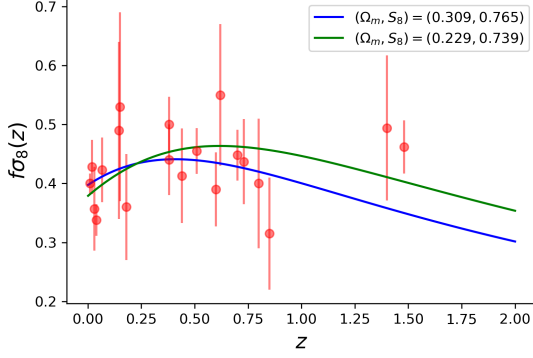
Figure 1. $f\sigma_8(z)$ constraints in red with best fit values of (Ω_m, S_8) both with (blue) and without (green) a Gaussian prior $\Omega_m = 0.3111 \pm 0.0056$.
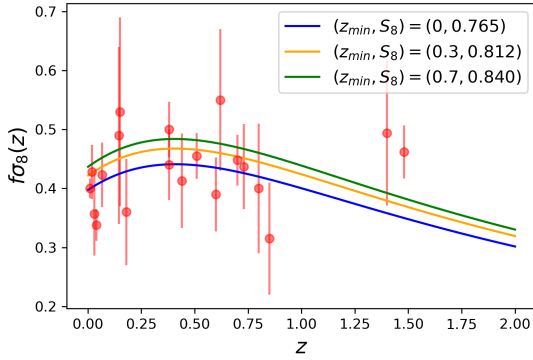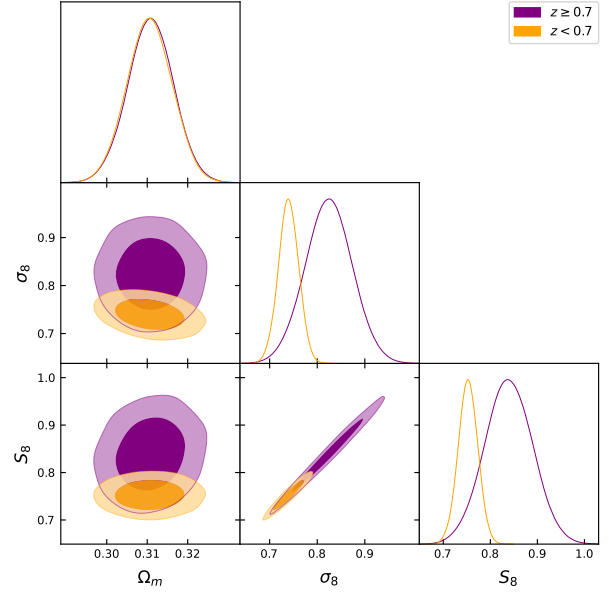

Figure 2. Same as Fig. 1 with Gaussian prior $\Omega_m = 0.3111 \pm 0.0056$ and data with $z \leq z_{\min}$ removed. S_8 increases with effective redshift.


Figure 3. Marginalisation of parameters $(\Omega_m, \sigma_8, S_8)$ with Gaussian prior $\Omega_m = 0.3111 \pm 0.0056$ and compilation of $f\sigma_8(z)$ data split at $z = 0.7$. S_8 is reconstructed from (Ω_m, σ_8) MCMC chains. The discrepancy in the S_8 plane between low and high redshift subsamples is 1.6σ.

driven by the two high redshift data points and is expected, since it is visible in the raw data, i. e. no data analysis is required. Note, the eBOSS data point at $z \sim 1.5$ is re-analysed in Brieden et al. (2022) with different methodology and the central point evolves little. There is nothing to suggest this data point is not robust.

We next split the $f\sigma_8(z)$ data at $z = 0.7$ into a low redshift sample of 14 data points and a high redshift sample of 6 data points. This choice is arbitrary, but it is guided by Fig. 1 and the intuition that evolution in S_8 is expected once we see evolution in H_0 Wong et al. (2020); Millon et al. (2020); Krishnan et al. (2020); Dainotti et al. (2021, 2022); Ó Colgáin et al. (2022); Ó Colgáin et al. (2022); Malekjani et al. (2023) and Ω_m Ó Colgáin et al. (2022); Ó Colgáin et al. (2022); Malekjani et al. (2023) elsewhere. We impose the Gaussian prior on Ω_m to each sample and perform a Markov Chain Monte Carlo (MCMC) analysis. The result is shown in Fig. 3, where in line with expectations from Fig. 2, the contours separate in the σ_8 or S_8 direction. The contours are Gaussian, allowing us to directly compare $S_8 = 0.753^{+0.021}_{-0.020}$ ($z < 0.7$) to $S_8 = 0.839^{+0.051}_{-0.050}$ ($z \geq 0.7$) and conclude that the discrepancy in S_8 is 1.6σ. Furthermore, the former value is discrepant with the Planck value $S_8 = 0.832 \pm 0.013$ Aghanim et al. (2020) at 3.2σ. Throughout, we quote 1σ confidence intervals. Note that the 1.6σ shift occurs within the 20 data point sample, which simply assumes that BAO and CMB can consistently constrain Ω_m. Observe also that the effect of the shift is to remove a $\sim 3\sigma$ tension with Planck in the S_8 parameter.

In Fig. 4, we investigate the effect of removing the Ω_m prior.

The low redshift sample leads to (Ω_m, σ_8) values consistent within 1σ with Planck, $(\Omega_m, \sigma_8) = (0.257^{+0.058}_{-0.051}, 0.803^{+0.088}_{-0.073})$, however $S_8 = 0.744^{+0.022}_{-0.022}$ is discrepant at 3.4σ. We emphasise that we sample (Ω_m, σ_8), but reconstruct S_8 as a derived parameter from the MCMC chains. The higher redshift contours are shifted away from their Planck values by more than 1σ throughout, $(\Omega_m, \sigma_8, S_8) = (0.124^{+0.117}_{-0.055}, 0.913^{+0.120}_{-0.084}, 0.585^{+0.172}_{-0.101})$, but remain consistent within 2σ. It is clear that lower values of S_8 are driven by lower than expected values of Ω_m in both low and high redshift subsamples. Note that caution is required when interpreting these shifts in the absence of an informative prior, as the high redshift sample is small with only 6 data points. In Fig. 5, we demonstrate the consistency between the Ω_m prior and the confidence intervals from low and high redshift samples in the (Ω_m, S_8)-plane. The intersection of the prior 1σ confidence interval explains the preference for the higher S_8 value from the high redshift subsample. Since all constraints are within 2σ, no objection to combining the constraints is foreseen. While removing the Ω_m prior makes a considerable difference, it is nevertheless true that we see less tension with Planck in the high redshift sample following shifts in cosmological parameters.

As an aside, with an Ω_m prior, we note that the ΛCDM model is still preferred over any theoretically poorly motivated model with a jump in σ_8 at $z = 0.7$. The reduction in the minimum of the χ^2, $\Delta\chi^2_{\min} = -2.59$ is not enough to overcome the penalty of introducing two additional parameters, an additional σ_8 and a redshift for the jump z_{jump}, even in the Akaike Information Criterion (AIC). Our observation here is essentially a microcosm of the ΛCDM tensions debate; despite seeing symptoms of a problem, here evolution in S_8 when $f\sigma_8(z)$ constraints are combined with CMB+BAO, it is a separate matter to produce a model that outperforms ΛCDM.

Given the relatively small size of the $f\sigma_8(z)$ data set considered in this work, in the appendix we work with a larger data set of historical data. The shortcomings of this data set are explicitly discussed, but we arrive at similar conclusions.
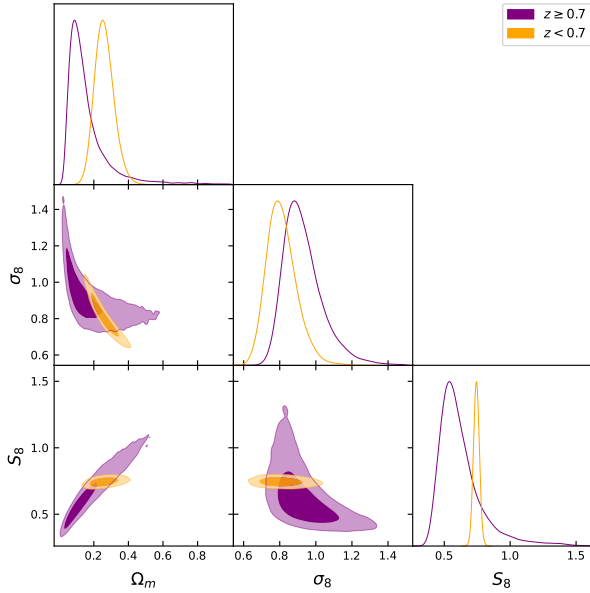
Figure 4. Same as Fig. 3 but without a Ω_m prior.
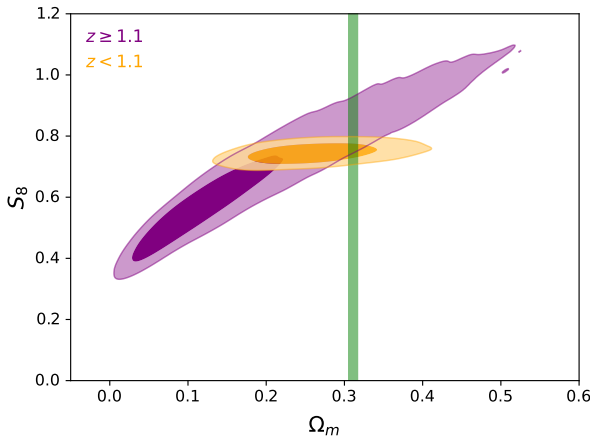
Figure 5. The CMB+BAO prior $\Omega_m = 0.3111 \pm 0.0056$ intersects the confidence intervals at larger values of Ω_m resulting in a larger value of S_8 in the high redshift ($z \geq 1.1$) sample. The prior is consistent with low and high redshift constraints within 2σ, so constraints can be safely combined.

3 CONCLUSIONS

Either from the Friedmann equations directly, or the continuity equation and the assumption of pressure-less matter, both H_0 and Ω_m arise *mathematically* as integration constants. Thus, consistency demands that both H_0 and Ω_m are *observationally* constants. An important corollary is that CMB, BAO, Type Ia supernovae, etc, must provide consistent Ω_m constraints in ΛCDM cosmology. Similarly, the fitting parameter σ_8 must be a constant, as it is related to the normalisation of the matter power spectrum. Here, working within the assumption that CMB and BAO consistently constrain Ω_m, we have shown that the $S_8 := \sigma_8 \sqrt{\Omega_m/0.3}$ parameter increases with effective redshift in the late Universe, $z \lesssim 2$. This evolution is compelling because it corroborates the tendency of cosmic shear to give lower values of S_8 than Planck-ΛCDM Aghanim et al. (2020); Heymans et al. (2013); Joudaki et al. (2017); Troxel et al. (2018); Hikage et al. (2019); Asgari et al. (2021); Abbott et al. (2022). Moreover, it is not an isolated

observation; we note that i) σ_8 constraints from low redshift clusters are biased lower than high redshift Lyman-α spectra Esposito et al. (2022) and ii) weak lensing S_8 constraints, sensitive to lower redshifts, are biased lower than CMB lensing results Qu et al. (2023); Madhavacheril et al. (2023); Marques et al. (2023) that are sensitive to higher redshifts. In Esposito et al. (2022); Qu et al. (2023); Madhavacheril et al. (2023); Marques et al. (2023), systematics are a greater concern as one is comparing different observables, but here we are working with common $f\sigma_8(z)$ constraints throughout, so systematics should be under greater control. The data largely comprises RSD but peculiar velocity constraints may be present at $z \sim 0$, e. g. Boruah et al. (2020); Said et al. (2020). However, these differences aside, we agree on the increasing σ_8 trend, a trend that is evident from the raw data.

It is instructive to recall the assumptions being made:

(i) Equation (3) is a valid approximation for ΛCDM behaviour.
(ii) Ω_m in ΛCDM is approximately 0.3.
(iii) Data sets and/or priors from independent data sets can be combined.
(iv) The data are correct.

If this set of assumptions is correct, then the increasing σ_8/S_8 trend follows. Assumption i) is standard Wang & Steinhardt (1998) and the theoretical uncertainty introduced is less than 1%, more accurately 0.2% in the redshift range $0.35 \lesssim z \lesssim 2$. Assumption ii) is a widely recognised observation. Assumption iii) is standard practice. Assumption iv) is the weakest, but the removal of data points requires justification. In other words, removing data points with the sole motivation of recovering a null result is unscientific.

Concretely, we presented analysis in a sample of 20 and 66 $f\sigma_8(z)$ (see appendix for the latter) constraints respectively. In both samples we find the same increasing S_8 trend, which is essentially a σ_8 trend, because Ω_m is subject to a strong prior. Since there is considerable survey overlap in Fig. A3, the tension between low and high redshift is admittedly *overestimated* at 2.8σ (Fig. A3). That being said, if the 20 data points in Fig. 1 are independent (Ref. Nguyen et al. (2023) assumes they are), then there is a 1.6σ shift in S_8 that warrants further study, especially since it seems to ameliorate tension with Planck. One could identify other redshift ranges where the discrepancy between low and high redshift inferences is less, but such an exercise is meaningless. To stress test any sample against evolution, one needs to focus on splits that exacerbate the feature. Moreover, Fig. A2 clearly demonstrates that evolution is present throughout the sample. Despite the presence of evolution, we find that the ΛCDM model is still preferred over any theoretically ad hoc model with a jump in S_8. Finally, when removing the Ω_m prior, despite noticeable differences in cosmological parameters, we find that high redshift data is more consistent with Planck.

Forthcoming releases from the Dark Energy Spectroscopic Instrument (DESI) DESI Collaboration et al. (2016) will be in a position to confirm or refute our assumption iv). Thus, our result is preliminary. Our findings also provide a targeted prediction for tomographic studies of cosmic shear Hikage et al. (2019); Asgari et al. (2021); Abbott et al. (2022). These surveys, i. e. HSC, KiDS and DES, currently employ redshift bins with varying effective redshifts across the surveys and shifts in cosmological parameters up to 1σ are evident. Given our results here, it is plausible that S_8 redshift evolution will be detected as cosmic shear data quality improves through a better understanding of systematics. If redshift evolution is not detected, and assuming S_8 tension is physical, then there must be evolution with scale Marques et al. (2023). Finally, our results caution theoretically that physics that alters the radius of the sound horizon Knox &

Millea (2020) cannot account for these *expected* hallmarks of model breakdown.

ACKNOWLEDGEMENTS

DATA AVAILABILITY

All the data analysed in this study are in the public domain and references are provided.

REFERENCES

Abbott T. M. C., et al., 2022, Phys. Rev. D, 105, 023520
Abdalla E., et al., 2022, JHEAp, 34, 49
Adams N. J., et al., 2022, Monthly Notices of the Royal Astronomical Society, 518, 4755
Addison G. E., Huang Y., Watts D. J., Bennett C. L., Halpern M., Hinshaw G., Weiland J. L., 2016, Astrophys. J., 818, 132
Aghanim N., et al., 2020, Astron. Astrophys., 641, A6
Alam S., et al., 2017, Mon. Not. Roy. Astron. Soc., 470, 2617
Alam S., et al., 2021, Phys. Rev. D, 103, 083533
Alonso D., Fabbian G., Storey-Fisher K., Eilers A.-C., García-García C., Hogg D. W., Rix H.-W., 2023, arXiv e-prints, p. arXiv:2306.17748
Asgari M., et al., 2021, Astron. Astrophys., 645, A104
Battye R. A., Charnock T., Moss A., 2015, Phys. Rev. D, 91, 103508
Bautista J. E., et al., 2020, Mon. Not. Roy. Astron. Soc., 500, 736
Benisty D., 2021, Phys. Dark Univ., 31, 100766
Beutler F., et al., 2012, Mon. Not. Roy. Astron. Soc., 423, 3430
Beutler F., et al., 2017, Mon. Not. Roy. Astron. Soc., 466, 2242
Blake C., et al., 2011, Mon. Not. Roy. Astron. Soc., 415, 2876
Blake C., et al., 2012, Mon. Not. Roy. Astron. Soc., 425, 405
Blake C., et al., 2013, Mon. Not. Roy. Astron. Soc., 436, 3089
Blakeslee J. P., Jensen J. B., Ma C.-P., Milne P. A., Greene J. E., 2021, Astrophys. J., 911, 65
Boruah S. S., Hudson M. J., Lavaux G., 2020, Mon. Not. Roy. Astron. Soc., 498, 2703
Brieden S., Gil-Marín H., Verde L., 2022, JCAP, 08, 024
Castellano M., et al., 2022, The Astrophysical Journal Letters, 938, L15
Chuang C.-H., Wang Y., 2013, Mon. Not. Roy. Astron. Soc., 435, 255
Chuang C.-H., et al., 2016, Mon. Not. Roy. Astron. Soc., 461, 3781
DESI Collaboration et al., 2016, arXiv e-prints, p. arXiv:1611.00036
Dainotti M. G., De Simone B., Schiavone T., Montani G., Rinaldi E., Lambiase G., 2021, Astrophys. J., 912, 150
Dainotti M. G., De Simone B., Schiavone T., Montani G., Rinaldi E., Lambiase G., Bogdan M., Ugale S., 2022, Galaxies, 10, 24
Davis M., Nusser A., Masters K., Springob C., Huchra J. P., Lemson G., 2011, Mon. Not. Roy. Astron. Soc., 413, 2906

Di Valentino E., Melchiorri A., Silk J., 2019, Nature Astron., 4, 196
Di Valentino E., et al., 2021, Class. Quant. Grav., 38, 153001
Esposito M., Iršič V., Costanzi M., Borgani S., Saro A., Viel M., 2022, Mon. Not. Roy. Astron. Soc., 515, 857
Feix M., Nusser A., Branchini E., 2015, Phys. Rev. Lett., 115, 011301
Feix M., Branchini E., Nusser A., 2017, Mon. Not. Roy. Astron. Soc., 468, 1420
Freedman W. L., 2021, Astrophys. J., 919, 16
Gil-Marín H., Percival W. J., Verde L., Brownstein J. R., Chuang C.-H., Kitaura F.-S., Rodríguez-Torres S. A., Olmstead M. D., 2017, Mon. Not. Roy. Astron. Soc., 465, 1757
Gil-Marín H., et al., 2018, Mon. Not. Roy. Astron. Soc., 477, 1604
Granett B. R., Neyrinck M. C., Szapudi I., 2008, Astrophys. J. Lett., 683, L99
Handley W., 2021, Phys. Rev. D, 103, L041301
Hawken A. J., et al., 2017, Astron. Astrophys., 607, A54
Heymans C., et al., 2013, Mon. Not. Roy. Astron. Soc., 432, 2433
Hikage C., et al., 2019, Publ. Astron. Soc. Jap., 71, 43
Hou J., et al., 2018, Mon. Not. Roy. Astron. Soc., 480, 2521
Hou J., et al., 2020, Mon. Not. Roy. Astron. Soc., 500, 1201
Howlett C., Ross A., Samushia L., Percival W., Manera M., 2015, Mon. Not. Roy. Astron. Soc., 449, 848
Howlett C., et al., 2017, Mon. Not. Roy. Astron. Soc., 471, 3135
Hu J.-P., Wang F. Y., 2022, Mon. Not. Roy. Astron. Soc., 517, 576
Hudson M. J., Turnbull S. J., 2013, Astrophys. J. Lett., 751, L30
Huterer D., Shafer D., Scolnic D., Schmidt F., 2017, JCAP, 05, 015
Jia X. D., Hu J. P., Wang F. Y., 2023, Astron. Astrophys., 674, A45
Joudaki S., et al., 2017, Mon. Not. Roy. Astron. Soc., 465, 2033
Kazantzidis L., Perivolaropoulos L., 2018, Phys. Rev. D, 97, 103503
Khadka N., Ratra B., 2020, Mon. Not. Roy. Astron. Soc., 497, 263
Khadka N., Ratra B., 2021, Mon. Not. Roy. Astron. Soc., 502, 6140
Khadka N., Ratra B., 2022, Mon. Not. Roy. Astron. Soc., 510, 2753
Knox L., Millea M., 2020, Phys. Rev. D, 101, 043533
Kourkchi E., Tully R. B., Anand G. S., Courtois H. M., Dupuy A., Neill J. D., Rizzi L., Seibert M., 2020, Astrophys. J., 896, 3
Kovács A., et al., 2017, Mon. Not. Roy. Astron. Soc., 465, 4166
Kovács A., et al., 2019, Mon. Not. Roy. Astron. Soc., 484, 5267
Kovács A., Beck R., Smith A., Rácz G., Csabai I., Szapudi I., 2022, Mon. Not. Roy. Astron. Soc., 513, 15
Krishnan C., Mondol R., 2022, arXiv e-prints, p. arXiv:2201.13384
Krishnan C., Ó Colgáin E., Ruchika Sen A. A., Sheikh-Jabbari M. M., Yang T., 2020, Phys. Rev. D, 102, 103525
Krishnan C., Ó Colgáin E., Sheikh-Jabbari M. M., Yang T., 2021, Phys. Rev. D, 103, 103509
Labbé I., et al., 2023, Nature, 616, 266
Li E.-K., Du M., Zhou Z.-H., Zhang H., Xu L., 2021, Mon. Not. Roy. Astron. Soc., 501, 4452
Lusso E., et al., 2020, Astron. Astrophys., 642, A150
Macaulay E., Wehus I. K., Eriksen H. K., 2013, Phys. Rev. Lett., 111, 161301
Madhavacheril M. S., et al., 2023, arXiv e-prints, p. arXiv:2304.05203
Malekjani M., Mc Conville R., Ó Colgáin E., Pourojaghi S., Sheikh-Jabbari M. M., 2023, arXiv e-prints, p. arXiv:2301.12725
Marques G. A., et al., 2023, arXiv e-prints, p. arXiv:2306.17268
Millon M., et al., 2020, Astron. Astrophys., 639, A101
Miyatake H., et al., 2022, Phys. Rev. Lett., 129, 061301
Mohammad F. G., et al., 2018, Astron. Astrophys., 610, A59
Naidu R. P., et al., 2022, The Astrophysical Journal Letters, 940, L14
Nesseris S., Pantazis G., Perivolaropoulos L., 2017, Phys. Rev. D, 96, 023542
Neveux R., et al., 2020, Mon. Not. Roy. Astron. Soc., 499, 210
Nguyen N.-M., Huterer D., Wen Y., 2023, Phys. Rev. Lett., 131, 111001
Nunes R. C., Vagnozzi S., 2021, Mon. Not. Roy. Astron. Soc., 505, 5427
Ó Colgáin E., Sheikh-Jabbari M. M., Solomon R., Bargiacchi G., Capozziello S., Dainotti M. G., Stojkovic D., 2022, Phys. Rev. D, 106, L041301
Ó Colgáin E., Sheikh-Jabbari M. M., Solomon R., Dainotti M. G., Stojkovic D., 2022, arXiv e-prints, p. arXiv:2206.11447
Okumura T., et al., 2016, Publ. Astron. Soc. Jap., 68, 38
Pastén E., Cárdenas V. H., 2023, Phys. Dark Univ., 40, 101224
Perivolaropoulos L., Skara F., 2022, New Astron. Rev., 95, 101659
Perlmutter S., et al., 1999, The Astrophysical Journal, 517, 565

Pesce D. W., et al., 2020, Astrophys. J. Lett., 891, L1

Pezzotta A., et al., 2017, Astron. Astrophys., 604, A33

Pourojaghi S., Zabihi N. F., Malekjani M., 2022, Phys. Rev. D, 106, 123523

Qu F. J., et al., 2023, arXiv e-prints, p. arXiv:2304.05202

Quelle A., Maroto A. L., 2020, Eur. Phys. J. C, 80, 369

Riess A. G., et al., 1998, Astron. J., 116, 1009

Riess A. G., et al., 2022, Astrophys. J. Lett., 934, L7

Risaliti G., Lusso E., 2019, Nature Astron., 3, 272

Said K., Colless M., Magoulas C., Lucey J. R., Hudson M. J., 2020, Mon. Not. Roy. Astron. Soc., 497, 1275

Samushia L., Percival W. J., Raccanelli A., 2012, Mon. Not. Roy. Astron. Soc., 420, 2102

Sanchez A. G., et al., 2014, Mon. Not. Roy. Astron. Soc., 440, 2692

Shi F., et al., 2018, Astrophys. J., 861, 137

Skara F., Perivolaropoulos L., 2020, Phys. Rev. D, 101, 063521

Song Y.-S., Percival W. J., 2009, JCAP, 10, 004

Tojeiro R., et al., 2012, Mon. Not. Roy. Astron. Soc., 424, 2339

Troxel M. A., et al., 2018, Phys. Rev. D, 98, 043528

Turnbull S. J., Hudson M. J., Feldman H. A., Hicken M., Kirshner R. P., Watkins R., 2012, Mon. Not. Roy. Astron. Soc., 420, 447

Turner R. J., Blake C., Ruggeri R., 2022, Mon. Not. Roy. Astron. Soc., 518, 2436

Wang L.-M., Steinhardt P. J., 1998, Astrophys. J., 508, 483

Wang Y., Zhao G.-B., Chuang C.-H., Pellejero-Ibanez M., Zhao C., Kitaura F.-S., Rodriguez-Torres S., 2018, Mon. Not. Roy. Astron. Soc., 481, 3160

Wilson M. J., 2017, PhD thesis, Edinburgh U. (arXiv:1610.08362)

Wong K. C., et al., 2020, Mon. Not. Roy. Astron. Soc., 498, 1420

Yang T., Banerjee A., Ó Colgáin E., 2020, Phys. Rev. D, 102, 123532

Zhao G.-B., et al., 2019, Mon. Not. Roy. Astron. Soc., 482, 3497

de Mattia A., et al., 2021, Mon. Not. Roy. Astron. Soc., 501, 5616

de la Torre S., et al., 2013, Astron. Astrophys., 557, A54

de la Torre S., et al., 2017, Astron. Astrophys., 608, A44

This paper has been typeset from a TEX/LATEX file prepared by the author.

APPENDIX A: LARGER ARCHIVAL DATA SET

Given that the increase in S_8 in the text is driven exclusively by two high redshift data points, it is prudent to work with a larger data set. The role of the second data set is to provide a sanity check, since the larger data set comes with caveats that we discuss below. To that end, we focus on Table II of Kazantzidis & Perivolaropoulos (2018), where one finds 63 historical measurements of $f\sigma_8(z)$ Beutler et al. (2012); Blake et al. (2013); Howlett et al. (2015); Okumura et al. (2016); Huterer et al. (2017); Song & Percival (2009); Blake et al. (2012); Davis et al. (2011); Hudson & Turnbull (2013); Turnbull et al. (2012); Samushia et al. (2012); Tojeiro et al. (2012); de la Torre et al. (2013); Chuang & Wang (2013); Sanchez et al. (2014); Wang et al. (2018); Feix et al. (2015); Chuang et al. (2016); Alam et al. (2017); Beutler et al. (2017); Wilson (2017); Gil-Marín et al. (2017); Hawken et al. (2017); de la Torre et al. (2017); Pezzotta et al. (2017); Feix et al. (2017); Howlett et al. (2017); Mohammad et al. (2018); Shi et al. (2018); Gil-Marín et al. (2018); Hou et al. (2018); Zhao et al. (2019). We add more recent data from Bautista et al. (2020); de Mattia et al. (2021); Neveux et al. (2020) to increase the sample to 66 data points. We observe that Refs. Beutler et al. (2012); Blake et al. (2013); Howlett et al. (2015); Okumura et al. (2016); Huterer et al. (2017) are common to both data sets in Fig. 1 and Fig. A1. The other data points are the work of independent groups, but as cautioned in Kazantzidis & Perivolaropoulos (2018), most analyses of growth rate data, e.g. Nguyen et al. (2023), tend to pick 20 odd data points to counteract any overcounting of data. However, this choice of *independent* data points is largely subjective. Moreover, different studies make use of different fiducial cosmologies. To address this latter concern, we follow equation (2.6) of Nesseris et al. (2017) (see also Macaulay et al. (2013)) and correct for this choice of fiducial model by performing a rescaling by the combination $H(z)D_A(z)$, where $H(z)$ and $D_A(z)$ denote the Hubble parameter and angular diameter distance at a given z. This means that the data set is consistent with the Ω_m prior by
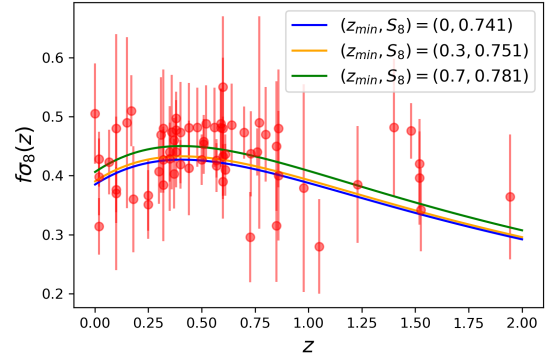
Figure A1. $f\sigma_8(z)$ constraints alongside best fit values of S_8 from fitting (3) in the range $z \geq z_{\min}$. Throughout we employ the Gaussian prior $\Omega_m = 0.3111 \pm 0.0056$.
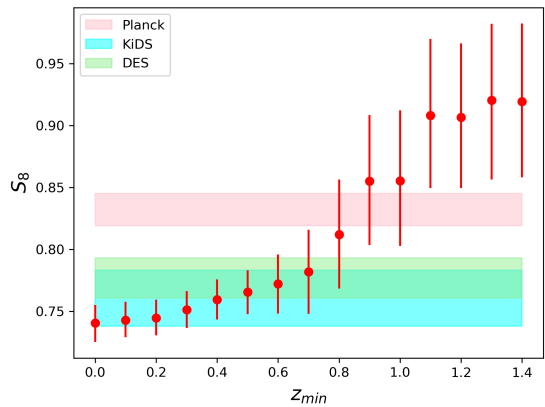

Figure A2. Removing $f\sigma_8(z)$ constraints with $z < z_{\min}$ while fitting expressions for the ΛCDM model (3) subject to a Gaussian prior $\Omega_m = 0.3111 \pm 0.0056$. An increasing S_8 trend with effective redshift is evident and the error bars correspond to 1σ confidence intervals. Constraints from KiDS, DES and Planck are illustrated for comparison.

construction. Note, following Nguyen et al. (2023), we did not perform this correction in the body of the letter. In the $f\sigma_8(z)$ literature, one finds groups who correct and do not correct for the fiducial cosmology.

In Fig. A2 we show the effect of removing $f\sigma_8(z)$ constraints below $z = z_{\min}$. Where relevant, e.g. WiggleZ Blake et al. (2012), we crop covariance matrices accordingly as we remove data points. Our strong Gaussian prior on Ω_m ensures that our *a posteriori* distributions from MCMC analysis remain Gaussian. As a result, the 1σ errors in Fig. A2 are representative. The reader will note that, in line with expectations, the size of the error bar increases as we remove data. Furthermore, the error bars in Fig. A2 are correlated, because all plotted constraints larger than a given $z_{\min}$ share data points.

We can address criticism regarding the correlated constraints in Fig. A2 by simply splitting the sample into independent subsamples. Our results in Fig. A2 suggest that any split at $z \sim 1$ may maximise the discrepancy between low redshift and high redshift subsamples. Once again, the trend is directly visible in the data in Fig. A1, since 7 from 8 data points above $z = 1$ prefer larger values of S_8/σ_8 than the full sample ($z_{\min} = 0$). The choice of split is somewhat arbitrary, as it depends on the composition or makeup of the overall sample, notably redshift distribution and quality of the data. For this reason, the split here is conducted at $z = 1.1$, whereas it was $z = 0.7$ in the body of the letter. Note that our sample here now has an extended range, so we can explore higher redshift splits of the sample. Concretely, we find that a split at $z = 1.1$ leads to $S_8 = 0.732 \pm 0.014$ at lower redshifts and
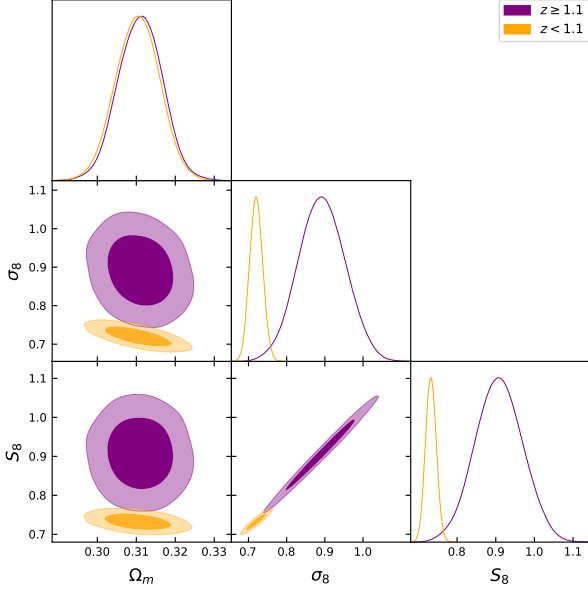
Figure A3. Marginalisation of parameters (Ω_m, σ_8, S_8) with Gaussian prior $\Omega_m = 0.3111 \pm 0.0056$ and compilation of $f\sigma_8(z)$ data split at $z = 1.1$. S_8 is reconstructed from (Ω_m, σ_8) MCMC chains. The discrepancy in the S_8 plane between low and high redshift subsamples is 2.8σ.
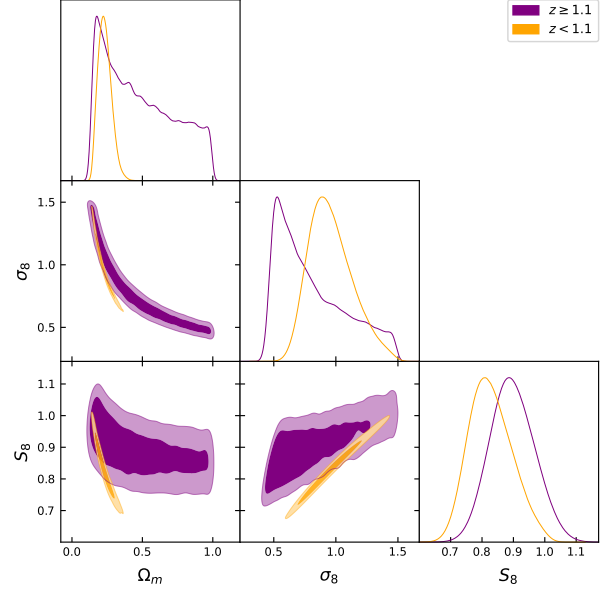
Figure A4. Same as Fig. A3 but without the CMB+BAO Ω_m prior. The 2D posterior in the (Ω_m, σ_8)-plane points to a degeneracy that is poorly broken by higher redshift constraints since the 1σ confidence intervals saturate the bounds.

$S_8 = 0.908 \pm 0.062$ at higher redshifts, with a tension at 2.8σ as illustrated in Fig. A3. Once again, it is worth noting that S_8 from data below $z = 1.1$ is in tension with Planck at $\sim 5\sigma$, while the data above $z = 1.1$ is consistent with Planck at $\sim 1\sigma$.

Removing the Ω_m prior, the corresponding results are $(\Omega_m, S_8) = (0.229^{+0.051}_{-0.044}, 0.823^{+0.077}_{-0.064})$ $(z < 1.1)$ and $(\Omega_m, S_8) = (0.435^{+0.352}_{-0.227}, 0.894^{+0.075}_{-0.068})$ $(z \geq 1.1)$. Evidently, all inferences are now consistent with Planck within 2σ, however as can be seen from Fig. A4, there is degeneracy in the (Ω_m, σ_8)-plane that the data fails to break. Thus, care needs to be taken with these inferences as they will be prior dependent. Noting that Ω_m is lower than expected in the lower redshift subsample, it is interesting to studying the full sample without the Ω_m prior. Doing, so we find $(\Omega_m, \sigma_8, S_8) = (0.191^{+0.035}_{-0.029}, 1.118^{+0.185}_{-0.158}, 0.890^{+0.066}_{-0.059})$. Evidently there is some discrepancy with Planck, whereby Ω_m, σ_8 and S_8 are respectively 3.5σ, 1.9σ and 1σ away. In both data sets considered in this work, there is evidently tension with Planck in one of the parameters.

Bearing in mind that not all the data points are independent, and as a result the errors are underestimated, the main take away from our analysis here is that the S_8 trend with Planck+BAO Ω_m prior is robust to changes in the data set. A secondary take away is confirmation that one expects to run into trouble in higher redshift bins without an Ω_m prior in line with equations (2) and (3).